Numerical Weather Prediction

The MOGREPS short-range ensemble prediction system Part I: System description

NWP Technical Report No. 497

Neill E. Bowler, Alberto Arribas, Kenneth R. Mylne & Kelvyn B. Robertson

email:nwp_publicationsmetoffice.gov.uk

© Crown copyright

The MOGREPS short-range ensemble prediction system Part I: System description

Neill E. Bowler* Alberto Arribas, Kenneth R. Mylne & Kelvyn B. Robertson

Met Office, FitzRoy Road, Exeter, EX1 3PB, UK.

Abstract:

The Met Office has recently introduced a short-range ensemble prediction system known as MOGREPS. This system consists of global and regional ensembles, with the global ensemble providing the boundary conditions and initial condition perturbations for the regional ensemble. Perturbations to the initial conditions are calculated using the Ensemble Transform Kalman Filter (ETKF), which is a computationally efficient version of the Ensemble Kalman Filter. Model uncertainties are represented in the system through a series of schemes designed to tackle the structural and sub-grid-scale sources of model error.

This paper describes the setup of the system and provides justification for the initial condition and model perturbation schemes chosen. An outline of the structure of the perturbations generated by the system is presented. Performance results, including verification from case studies and routine running, are described in a companion paper.

Crown Copyright © 2007

KEY WORDS ensemble forecasting short-range NWP

*Correspondence to: N. E. Bowler, Met Office, FitzRoy Road, Exeter, EX1 3PB, UK. E-mail: Neill.Bowler@metoffice.gov.uk

Crown Copyright © 2007

1 Introduction and Motivation

Ensemble forecasting has proved to be a successful way of dealing with the inherent uncertainty of weather and climate forecasts (Buizza *et al.*, 2005). After more than a decade of running operationally, ensemble prediction systems (EPS) for the medium-range, such as those run at the European Centre for Medium Range Weather Forecasts (ECMWF) or the US National Centers for Environmental Prediction (NCEP), can now be considered as mature systems. These systems are designed for forecast lead times of 3 to 10 days and mainly focus on the uncertainties due to synoptic-scale baroclinic instability. However, significant forecast uncertainty also occurs on shorter time and length scales. On rare but critically important occasions there is significant uncertainty in large-scale developments - the most common example, affecting Europe in most years, is rapid cyclogenesis which leads to some of the most significant and intense autumn and winter storms. Much more commonly there is large uncertainty in the local details of the weather which are of interest to many forecast users on a daily basis, such as temperature and wind speed, timing or location of precipitation systems, QPF (quantitative precipitation forecasts), precipitation type (eg. rain or snow), low cloud and visibility. There is now increasing interest in developing ensemble prediction systems to address these short-range uncertainties.

In order to adequately tackle forecast uncertainty on short time scales, there are three key requirements for an ensemble system:

1. A higher-resolution model than those typically used for the medium-range. Limited computer resources restrict the resolution of global ensembles to grid-lengths of order 50-100km at mid-latitudes. To address many of the uncertainties above requires higher resolutions for which it is necessary to run limited-area models (LAMs).
2. Perturbations to the initial condition (IC) need to be effective immediately from the initial time which means that they should focus on quantifying the uncertainties in the analysis. Some approaches which are effective in medium-range EPS may be less appropriate for use very close to initialisation time. In particular, the singular vector (SV) approach used at ECMWF (Buizza and Palmer, 1995; Molteni *et al.*, 1996), which is optimised to grow the perturbations over the early part of the forecast period and so may not be suitable for short-range ensembles.
3. An approach to address uncertainties arising from model error is essential. Approximations in model formulation are unavoidable, for example due to unresolved atmospheric processes which must be parameterised. Errors arising from such uncertainties can be amplified during the course of the forecast, or can result in errors in derived forecast weather parameters. In fact, dealing with model error in ensembles is thought to be an even greater challenge than simulating initial condition perturbations (Buizza *et al.*, 2005).

This paper describes the development of MOGREPS (Met Office Global and Regional Ensemble Prediction System) which has been designed specifically to satisfy these requirements and provide a short-range ensemble prediction capability to meet the needs of Met Office customers. Over

Crown Copyright © 2007

recent years a number of regional EPSs have been developed, and before describing the MOGREPS approach we briefly review some of the methods employed elsewhere.

NCEP's SREF was the pioneering short-range ensemble developed out of research using a multi-model approach with two LAMs with boundary conditions taken from the NCEP medium-range global ensemble (Tracton *et al.*, 1998; Stensrud *et al.*, 1999). The SREF has since evolved such that it now runs 21 members using three different core models with horizontal grid lengths of between 32 and 45km. Several variants of the models are included using different parameterisation schemes to address model uncertainty. Breeding Vectors (BVs) (Toth and Kalnay, 1993) are used to create the perturbations to the initial conditions. The SREF is run quasi-operationally twice daily to 87 hours ahead.

The Spanish Met Service, INM, has developed a multi-model short-range ensemble over SW Europe employing five different regional models each run with four different analyses and lateral boundary conditions provided from different global Numerical Weather Prediction (NWP) centres (Garcia-Moya *et al.*, 2007). A similar system has been developed over the Pacific Northwest of the USA at the University of Washington (Eckel and Mass, 2005). In each case initial condition perturbations are provided by the analyses from different centres, which provides a sampling of the analysis uncertainty through the solutions reached by different operational quality control and analysis systems. Uncertainty due to model error is sampled through the use of multiple models, or model versions, within the ensembles. Eckel and Mass (2005) concluded that accounting for model uncertainty is most critical for surface weather variables over land.

The Norwegian Meteorological Institute, NMI, runs a 21-member regional ensemble, LAMEPS, over Scandinavia with a grid-length of 28km (Frogner *et al.*, 2006). Lateral boundary conditions and initial condition perturbations are provided from a version of the ECMWF EPS with singular vector perturbations targeted to maximise 48-hour growth over NW Europe (as opposed to the whole of the northern hemisphere in the standard ECMWF EPS). In the regional ensemble, perturbations are added to the high-resolution regional analysis. The regional approach is shown to be particularly effective over the mountainous areas of Norway where the high-resolution model is better able to predict the high-intensity precipitation events that are observed.

Meteo-France has developed a system known as PEACE (Jean Nicolau, personal communication). This ensemble is based on the stretched-grid ARPEGE model and has a resolution of approximately 20km over France. The system has 11 ensemble members (10 perturbed plus one control) and is run once per day to T+60 hours. Initial condition perturbations are computed using singular vectors optimised over a 12-hour window. Unlike the ECMWF ensemble, no evolved singular vectors are used, and no model uncertainty schemes are used.

The COSMO-LEPS ensemble (Marsigli *et al.*, 2004; Molteni *et al.*, 2001) provides a regional downscaling of the ECMWF EPS to provide enhanced resolution, particularly for orographically-forced intense precipitation. The EPS is sub-sampled by clustering into a number of clusters, currently 16, and "representative" members of each cluster are used to

Crown Copyright © 2007

provide the initial conditions and lateral boundary conditions for the members of the COSMO-LEPS ensemble. As initial condition perturbations are taken from the EPS they are optimised for the medium-range, so COSMO-LEPS is more appropriate for the early medium-range (2-5 days) than the short-range. All COSMO-LEPS members are integrated using the Lokal model of the COSMO consortium. A small amount of model diversity has recently been introduced to help account for model error by random selection between two alternative convective parameterisation schemes.

Figure 1. Map showing the domain of the Met Office's models. The NAE model covers much of the north Atlantic and Europe, and is shown in a darker shading here. Also shown is the UK meso-scale model area in a lighter colour.

The German Met Service, DWD, runs a so-called "poor-man's ensemble" known as SRNWP-PEPS (see page at http://www.dwd.de/en/FundE/Projekte/PEPS/index.htm) on behalf of the EUMETNET collaboration of European Met Services. This system combines the forecasts from the deterministic models of European forecast centres. Arribas *et al.* (2005) showed promising results for the short-range forecast with a similar system based on global models, and initial results from SRNWP-PEPS have also been encouraging (Martin Goeber, private communication).

This list is not intended to be comprehensive, focusing mainly on developments in Europe, but nevertheless illustrates that short-range ensemble prediction is developing rapidly in many centres. A variety of different approaches is employed to address some or all of the three requirements listed above, partly depending on the different facilities and requirements of centres. In developing MOGREPS we aimed to address all three requirements:

1. We use the North-Atlantic and European (NAE) regional version of the Met Office's Unified Model, illustrated in figure 1, with a horizontal grid-length of 24km and 38 levels in the vertical. This combination of domain and resolution is sufficient to resolve more detail in developing Atlantic weather systems than is available from medium-range global ensembles, but not sufficient for many fine-scale synoptic details. In order to ensure that consistent perturbations can be applied across the boundaries of the regional model, a global ensemble is run which produces the initial condition perturbations and lateral boundary conditions that are fed to the NAE ensemble.
2. Initial condition perturbations for MOGREPS are generated using an Ensemble Transform Kalman Filter (ETKF) (Bishop *et al.*, 2001). This may be thought of as a natural generalisation of the error breeding method (Toth and Kalnay, 1993), in which the perturbations determined for each cycle are a linear combination of the forecast perturbations from the previous cycle. This mixing allows the perturbations to be orthogonalised, and has been seen to lead to improved performance over error

Crown Copyright © 2007

breeding (Wang *et al.*, 2004). The ETKF provides a set of perturbations which are added to the Met Office 4D-Var analysis to provide the initial states for ensemble members. This is believed to be the first implementation of a quasi-operational EPS using the ETKF and taking account of the full set of observations used in the data-assimilation system used to provide the analysis.

3. Most other short-range ensembles described above have addressed model uncertainty through use of multiple models or multiple model versions, usually parameterisation schemes. One drawback of these methods is that ensemble members are systematically different from each other. Ensemble members are therefore expected to have different skills, hindering the extraction of probabilities from the ensemble. Ensemble members from this kind of system tend to cluster by model (Alhamed *et al.*, 2002), so that the form of a forecast ensemble pdf (probability density function) may be dictated more by the distribution of models/schemes than by the synoptically dependent forecast uncertainty. Multi-model or multi-parameterisation methods are also complex to maintain. To avoid these problems with MOGREPS, we set out to develop a system which would address model error within a single model environment using stochastic perturbations to the model, mainly to the parameterised model physics. The model used to integrate every member of the ensemble is therefore the same, apart from the choice of the number chosen to seed a random number generator. Two schemes are implemented. The Random Parameters (RP) scheme targets uncertainty due to structural sources of uncertainty caused by choice of tunable parameters inside the physical parameterisations. The Stochastic Convective Vorticity (SCV) scheme addresses uncertainty due to sub-grid-scale (i.e. not fully resolved) processes, in particular the impact of organised but unresolved convection. It is important to emphasise that uncertainties in initial condition and model are not independent, but intrinsically linked through the use of the model to provide the background state in data assimilation. This is represented in MOGREPS by the ETKF which propagates an estimate of model uncertainty from the above schemes into the initial condition perturbations for the next cycle.

Apart from the benefits of tackling forecast uncertainties in the short-range, MOGREPS will also allow us to address other scientific problems and long-term strategic aims. Forecast uncertainties from MOGREPS will be propagated through downstream models (e.g. hydrological models, storm surge models and severe weather impact models) to allow end-to-end probabilistic prediction of weather impact. Strategic aims include providing lateral boundary conditions (LBCs) for future convective-scale ensembles and generation of synoptically dependent background error covariance statistics for use in data assimilation.

The paper is organised as follows: The configuration of the system is described in Section 2. The perturbation method for the initial condition is

Crown Copyright © 2007

explained in Section 3. Section 4 is dedicated to describe the schemes representing model uncertainty. Summary and conclusions are presented in Section 5.

MOGREPS has been run in the Met Office operational suite since August 2005. A discussion of the performance and verification of the system is presented in a companion paper: "The MOGREPS short-range ensemble prediction system Part II: Case Studies, Performance and Verification".

2 System Configuration

MOGREPS consists of two ensembles, one global and one regional using a higher-resolution LAM centred on Europe (the NAE ensemble). The domain area requirements for the LAM were driven by the fact that many of the uncertainties important for NW Europe stem from developments in the Atlantic. Therefore, the domain, shown in figure 1, was chosen to be big enough to allow these systems to be well represented.

The resolution of both ensemble systems has been chosen to be approximately half the resolution of the corresponding deterministic models. The global ensemble is run at N144 resolution (approximately 90km in the mid-latitudes) with 38 vertical levels, which compares with N320 resolution and 50 levels (upgraded from N216 and 38 levels on 13 December 2005) for the deterministic global model. The NAE ensemble is run at 24km resolution and 38 vertical levels, which compares with 12km resolution and 38 vertical levels for the deterministic NAE model.

The run times of the ensembles are offset by 6 hours to distribute the computing burden more evenly through the day. The global ensemble runs at 0Z and 12Z and the NAE ensemble runs at 6Z and 18Z. Thus the NAE ensemble takes its LBCs and initial condition perturbations from a 6-hour forecast of the global ensemble. For a short-range ensemble to be useful in an operational framework it is critical that the forecasts are available as early as possible after data-time, and this arrangement allows the NAE ensemble to be run immediately after the new NAE analysis becomes available (rather than having to wait for the global ensemble to run first). Global MOGREPS forecasts are run to 72 hours ahead and NAE MOGREPS to 36 hours for results presented in these papers, although the latter has more recently been extended to 54 to fully encompass Day 2.

In many ensemble systems (such as those which use SVs or BVs) the quality of each perturbation is independent of the number of ensemble members. In these cases the rationale for increasing the number of ensemble members is to provide a better sampling of the forecast pdf. For the ETKF an increase in the number of ensemble members means that the rank-deficiency of the forecast error covariance matrix is reduced and the ensemble update becomes more accurate. Hence there is additional motivation for increasing the ensemble size. Wang and Bishop (2003) found a marked improvement in ETKF performance with 16 members compared to 8 members using only radiosonde observations to calculate the transform matrix and train the inflation factor, and suggested that a larger ensemble would be beneficial in accounting for variations in observation density. As with any operational system, the number of ensemble members in MOGREPS is a compromise between scientific and

Crown Copyright © 2007

technical reasons. In our case, it is beneficial to run using a number of ensemble members which is a multiple of 8, since each node of the Met Office supercomputer has 8 processors. We have chosen to use 24 ensemble members in both ensembles, global and regional. Each forecast takes around 45 minutes to complete on 2 processors of an NEC SX6.

3 Initial Condition Perturbations

For a short-range ensemble to be useful, it is a fundamental requirement that perturbations to the initial condition are valid from the initial time. This implies that the perturbations have to be focused on quantifying the uncertainties in the analysis; the ETKF is based on a data assimilation scheme and fulfills this requirement. During tests of varying ensemble schemes in a simple model environment (Bowler, 2006) the ensemble Kalman filter (EnKF) was seen to perform best. In MOGREPS we add the perturbations to the Met Office's operational 4D-Var analysis, so we do not require a full EnKF to update the ensemble mean analysis. The ETKF provides a fast and cheap calculation of the ensemble perturbations without updating the analysis, so is an appropriate way to gain many of the benefits of an EnKF without much of the computational expense.

In the current version of MOGREPS the NAE ensemble does not produce its own initial condition perturbations but derives them directly from those of the global ensemble. A description of the ETKF and how it derives from the Ensemble Kalman Filter follows.

3.1 Ensemble Kalman Filter (EnKF)

The Kalman filter (Bozic, 1979; Kalman, 1960) is a data assimilation scheme which provides an optimal estimate of the true state of the system given certain conditions. The filter works by maintaining an estimate of the true state, which is updated by a forecast of the state from the previous time and by observations. Errors in the observations, the state at the previous time and the model for propagating this state forward in time are accounted for. The filter provides an optimal data assimilation system if the model and observation operator are linear, and all the errors are Gaussian. These conditions are not met by Numerical Weather Prediction (NWP) models of the atmosphere. For NWP models the ensemble Kalman filter (Evensen, 1994) is a useful approximation of the Kalman filter, which allows the data assimilation to be computed on the basis of a limited-size ensemble. It still assumes that all the errors are Gaussian (which will not be the case when non-linear models are used) but behaves well even when they are not.

As input the EnKF requires an ensemble of forecasts of the current state from which the background error covariance may be estimated

$$\mathbf{P}^f = \frac{\mathbf{X}^f \mathbf{X}^{fT}}{K-1} \tag{1}$$

where K is the size of the ensemble and the columns of $\mathbf{X}^f$ correspond to the difference between an ensemble member and the ensemble mean forecast. A localisation function is often applied to $\mathbf{P}^f$ since the number of degrees of freedom in this matrix is vastly greater than the size of normal ensembles. The ensemble mean analysis may be calculated

Crown Copyright © 2007

using

$$\bar{\mathbf{x}}^a = \bar{\mathbf{x}}^f + \mathbf{G}\left(\mathbf{Y} - H\left(\bar{\mathbf{x}}^f\right)\right) \tag{2}$$

where $\bar{\mathbf{x}}^a$ is the ensemble mean analysis, $\bar{\mathbf{x}}^f$ is the ensemble mean forecast, $\mathbf{Y}$ are the observations, $H()$ is the observation operator and $\mathbf{G}$ is known as the Kalman gain, given by

$$\mathbf{G} = \mathbf{P}^f\mathbf{H}^T\left(\mathbf{H}\mathbf{P}^f\mathbf{H}^T + \mathbf{R}\right)^{-1} \tag{3}$$

where $\mathbf{R}$ is the observation error covariance matrix, and $\mathbf{H}$ is a linearised version of $H()$. The inversion of the term on the right of eq. 3 can be very expensive for NWP models which use large numbers of observations.

Equation 2 is correct for performing the update of the ensemble mean, or analysis, but to derive the correct distributions of analysis perturbations it would normally be necessary to perturb the observations, $\mathbf{Y}$. However, since $\mathbf{R}$ is often diagonal it may be appropriate to process the observations serially (Whitaker and Hamill, 2002). In this case $\mathbf{H}\mathbf{P}^f\mathbf{H}^T$ and $\mathbf{R}$ reduce to scalars. To update the perturbations without perturbing the observations $\mathbf{G}$ is multiplied by

$$\alpha = \left(1 + \sqrt{\frac{\mathbf{R}}{\mathbf{H}\mathbf{P}^f\mathbf{H}^T + \mathbf{R}}}\right)^{-1}. \tag{4}$$

This algorithm performs better than the standard EnKF with perturbed observations (Evensen, 2004).

3.2 Ensemble transform Kalman filter (ETKF)

The ensemble transform Kalman filter (ETKF) (Bishop *et al.*, 2001) is equivalent to the EnKF and allows for rapid calculation of the analysis perturbations. The ETKF is approximately 10^5 times faster than the serial EnKF for current NWP models. The efficiency of the computation relies on the analysis

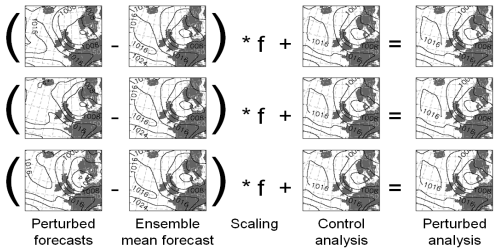

Figure 2. Graphical explanation of the error breeding method. Error breeding re-scales the perturbation for each member separately.

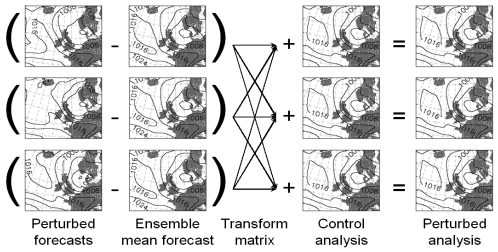

Figure 3. Graphical explanation of the ETKF method. The ETKF mixes the perturbations of different members via the transform matrix

perturbations being in the subspace of the forecast perturbations. Hence, covariance localisation is not possible within the ETKF framework. The scheme centres around calculating a transform matrix, $\mathbf{T}$, which transforms the forecast perturbations according to

$$\mathbf{X}^a = \mathbf{X}^f\mathbf{T}. \tag{5}$$

The analysis perturbations for a given variable are therefore a linear combination of the forecast perturbations for that variable. Thus, the ETKF may be seen as being closely related to the error breeding method - this is illustrated graphically in figures 2 & 3.

The transformation matrix may be calculated as (Wang *et al.*, 2004)

$$\mathbf{T} = \mathbf{C}(\Gamma + \mathbf{I})^{-1/2}\mathbf{C}^T \tag{6}$$

Crown Copyright © 2007

where $\mathbf{C}$ and Γ are derived from the eigenvectors and eigenvalues of the matrix

$$\mathbf{E} = \frac{\left(\mathbf{R}^{-1/2}H\left(\mathbf{X}^f\right)\right)^T\left(\mathbf{R}^{-1/2}H\left(\mathbf{X}^f\right)\right)}{K-1}. \quad (7)$$

Since $\mathbf{X}^f$ contains the ensemble perturbations (and therefore must sum to zero) one of the eigenvalues of $\mathbf{E}$ will be zero. Γ is a $(K-1)\times(K-1)$ diagonal matrix containing all the eigenvalues of $\mathbf{E}$ except this zero eigenvalue, and $\mathbf{C}$ contains the corresponding eigenvectors, save the one relating to the zero eigenvalue. The perturbations thus generated will be orthogonal to each other in the space of the observations (Wang *et al.*, 2004), and have the appropriate variance, as dictated by the Kalman filter formulation.

The sum of the perturbations to the analysis is guaranteed to be zero using the formulation of the transform matrix given in eq. 6. This is because the sum of $\mathbf{X}^f$ is defined to be zero, and $\mathbf{T}\mathbf{T}^T$ is a diagonal matrix.

The variance in an ensemble generated by an EnKF is often smaller than required due to the problems of inbreeding and covariance estimation based on small ensemble sizes (Houtekamer and Mitchell, 1998). This issue is particularly pertinent for the ETKF, since no covariance localisation is possible to alleviate this problem. We overcome this problem using a variable inflation factor, similar to that used by Wang and Bishop (2003). In their scheme the inflation factor for forecast cycle n is calculated according to the formula

$$\Pi_n = \Pi_{n-1}\sqrt{\frac{Tr(d_n d_n^T) - Tr(\mathbf{R})}{Tr(\mathbf{S}_n)}} \quad (8)$$

where $Tr()$ indicates the matrix trace, $d_n = \mathbf{Y} - H\left(\bar{\mathbf{x}}^f\right)$ is innovation vector, giving the error in the ensemble mean forecast and $\mathbf{S}_n = \mathbf{H}\mathbf{P}^f\mathbf{H}^T$ is the spread of the forecast ensemble in observational space for cycle n. Thus, this scheme seeks to ensure that the spread of the ensemble matches the error of the ensemble mean forecast (both at some lead time) accounting for the error in the observations. However, this scheme is unsatisfactory since it can introduce oscillations in the ensemble spread. Imagine that at cycle $n-1$ the ensemble spread is too small, and the inflation factor gives a large value. If for cycle n the ensemble spread now matches the error of the ensemble mean, then the large inflation factor will be used once more. Thus, for cycle $n+1$ the ensemble spread becomes too large and subsequent inflation factors will have to be small to reduce the spread. To avoid this problem, we use an inflation factor which is the geometric mean of the term in the square root of equation 8 and the ratio of the mean-square spread at times $n-1$ and n. The new inflation factor is thus

$$\Pi_n = \Pi_{n-1}\sqrt{\frac{[(Tr(d_n d_n^T) - Tr(\mathbf{R}))Tr(\mathbf{S}_{n-1})]^{\frac{1}{2}}}{Tr(\mathbf{S}_n)}}. \quad (9)$$

Figure 4 shows the inflation factors calculated using this scheme over a number of months of running. These have been calculated using only radio-sonde observations and use a 12-hour forecast. Our scheme may still be susceptible to the vagaries of the observational network, and we believe that it is this which gives the diurnal variation to the ensemble spread. By using only radio-sonde observations we hope that the estimates of the observational error that are used by the data assimilation system are accurate enough to give good performance. The

Crown Copyright © 2007

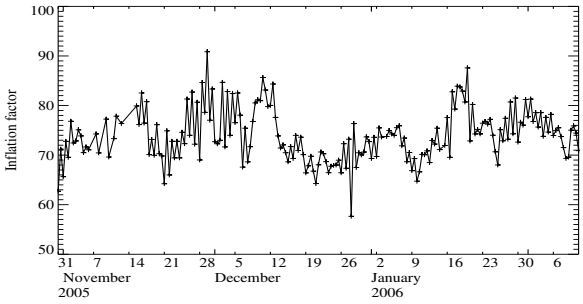

Figure 4. Inflation factors applied in the ETKF between 30 October 2005 and 15 Feb 2006. The system did not run on some days, so no values are provided for these dates.

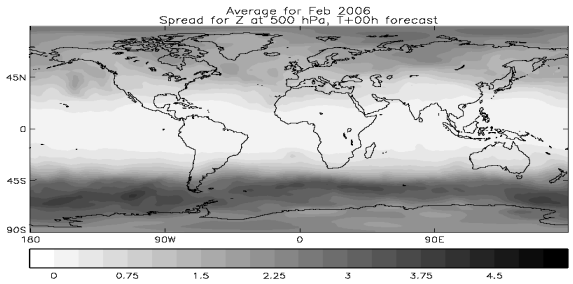

Figure 5. Spread of the ensemble at initial time, averaged for the month of February 2006 for 500 hPa height.

large magnitude of the inflation factors is due to spurious long-range correlations (attributable to limited ensemble size), inbreeding and an incomplete treatment of the model error. These values are consistent with previous studies (Wang *et al.*, 2004). Since the inflation is applied to the transform matrix, the perturbations do not change in size, but the inflation factor ensures that the entries of this matrix are of order one.

In previous implementations of the ETKF (Wang *et al.*, 2004; Wei *et al.*, 2006) only a limited set of observations were used in calculating the transform matrix. However, only the forward observation operator is required in eq. 7 so there is no restriction on the observations types used. We have chosen to include every observation used by the 4D-Var data assimilation scheme within the ETKF. This adds to the computational burden of the ETKF, since the radiative transfer calculations are costly, but should allow the ETKF to better represent the errors in the analysis used in this system.

3.3 Structure of ETKF perturbations

In previous studies (Wang *et al.*, 2004; Wei *et al.*, 2006) the similarity between the ETKF perturbations and bred perturbations has been noted. In both schemes the initial perturbations are much larger than those derived from the singular vectors method. This is illustrated in figure 5 which shows the spread of the ensemble at initial time, averaged for the month of February 2006. This may be (indirectly) compared with figure 2 of Wei *et al.* (2006) which is qualitatively very similar to the figure shown here. The spread is much larger for the extra-tropics than the tropics, and larger for the southern hemisphere than for the northern. The areas of large spread coincide with dynamically active regions. There is also some longitudinal variation of the spread, such as reduced spread over North America and Europe, which appears to coincide with well-observed regions.

The variation of the total energy density in the initial conditions perturbations with height is shown in figure 6 for ensemble perturbations on 1 February 2006. The energy density is calculated according to

$$E = \frac{1}{2}\rho\left(u'^2 + v'^2\right) + \frac{p}{2\kappa T_{ref}^2}T'^2 + \frac{1}{2\gamma p}p'^2 \qquad (10)$$

Crown Copyright © 2007

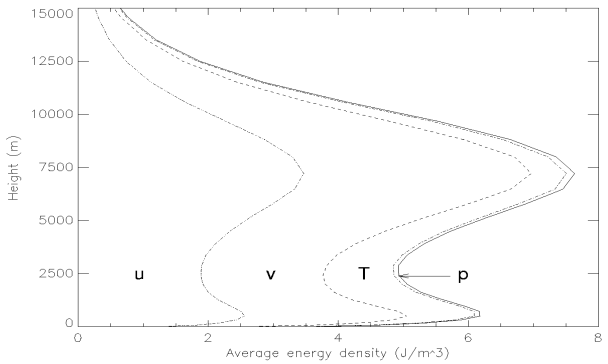

Figure 6. Average energy density of the initial conditions perturbations, partitioned into components for the different variables being perturbed. The distance between two lines indicates the energy density for a given variable.

where $\kappa = \frac{R}{C_p} \simeq 0.286$ and $\gamma = \frac{C_p}{C_v} \simeq 1.4$. The variables p and ρ are taken from the control forecast, and T_{ref} is a fixed reference temperature of 300K. This formula gives the kinetic and available potential energy for the perturbation (primed quantities) relative to the control forecast (unprimed quantities) in an ideal isothermal atmosphere. This calculation has been attempted using a formula appropriate for a non-isothermal atmosphere. In that case the energy attributed to the temperature perturbations was larger, but the formula gave erroneous results in the boundary layer. The greatest energy density in figure 6 is around 7km above the surface, which is slightly below the level of the jet. A secondary peak in the energy density occurs near the surface. The vast majority of the perturbation energy is in kinetic energy. The energy in the temperature perturbation does not peak in the same regions as u and v, with the maximum energy density being in the lower-mid-troposphere. The perturbations to the pressure and moisture (not shown) fields carry very little energy. The partition of the energy changes little as the forecast progresses.

4 Stochastic physics

Representation of model uncertainties is now considered indispensable in any ensemble system. In fact, it is hypothesised to be the major contributor to the under-dispersion observed in medium-range operational systems (Hamill and Colucci, 1997).

In MOGREPS, two stochastic physics schemes are included to represent the effects of structural and sub-grid-scale model uncertainties: the Random Parameters (RP) scheme and the Stochastic Convective Vorticity (SCV) scheme. The latter of these is used only by the global ensemble.

Crucially, the choice of using stochastic physics with a filtering method (ETKF) to specify the initial condition uncertainty means that the model perturbations influence the initial condition perturbations.

4.1 The Random Parameters (RP) scheme

There are many physical processes (convection, boundary layer exchanges, etc) that occur on scales too small to be directly resolved by the model and need to be parameterised. These parameterisations involve a number of empirical-adjustable parameters and thresholds which are given somewhat arbitrary values. The RP scheme aims to account for the uncertainty associated with these empirical parameters and to simulate the non-deterministic processes not explicitly accounted for by the different parameterisations.

The idea behind RP, to treat a selected group of parameters as stochastic variables, is similar to the approach followed by Lin and Neelin (2000) and Bright and Mullen (2002). Each parameter value is calculated using a first-order auto-regression model

Crown Copyright © 2007

(Wilks, 1995) as given by:

$$P_t = \mu + r\,(P_{t-1} - \mu) + \epsilon \tag{11}$$

where P_t is the parameter value at time t, μ is the mean value of the parameter, r is the autocorrelation of P and ϵ is the stochastic shock term.

A total of 8 parameters from 4 different physical parameterisations are included. The physical parameterisations affected by the scheme are: Large-scale precipitation (Wilson and Ballard, 1999), Convection (Gregory and Rowntree, 1990), Boundary Layer (Lock *et al.*, 2000) and Gravity Wave drag (Webster *et al.*, 2003). A brief description of each parameter follows:

- *Entrainment Rate Coefficient*: Scalar, part of the convection scheme. This parameter scales the rate of mixing between environmental air and the convective plume.
- *Time scale for destruction of CAPE*: Scalar, part of the closure of the convection scheme. It determines how intense the convective mass flux needs to be to eliminate the available CAPE in a given time.
- *Flux profile parameter*: Scalar, part of the stable boundary layer scheme. It determines the stability dependence of turbulent mixing coefficients, for example enhancing or reducing mixing in a stable boundary layer.
- *Asymptotic neutral mixing length*: Scalar, part of the boundary layer scheme. This parameter sets the magnitude of the mixing lengths and hence the turbulent mixing coefficients.
- *Gravity Wave constant*: Scalar, part of the Gravity wave drag scheme. It defines the magnitude of the parameterised response.
- *Critical Froude number*: Scalar, part of the gravity wave drag scheme. It determines the proportion of the drag attributed to flow blocking and gravity wave drag respectively. The larger the critical Froude number the larger the proportion attributed to flow blocking.
- *Critical relative humidity*: Vector, part of the large-scale precipitation scheme. This is the threshold of relative humidity for cloud formation. It takes different values on different model levels. In order to be consistent with the structure in the standard version of the model a value for the perturbation to the critical value at level 3 is calculated, and this perturbation is also applied to all levels above this. The critical values used at the bottom two levels of the model are not perturbed.
- *Ice fall speed parameter*: Scalar, part of the large scale precipitation scheme. The ice fall speed is modified by this parameter.

In order to avoid unrealistic values, each parameter is bound by minimum and maximum values P_{min} and P_{max} which were estimated by experts in each field (see values in Table I). The stochastic shock term, ϵ, is sampled from a uniform distribution from the range $\pm(P_{max} - P_{min})/3$. This is an arbitrary choice, but a uniform distribution was preferred over a normal distribution to avoid the values being constrained towards a mean value. The autocorrelation r has been given a value of 0.95 and the parameters' values are updated every 3-hours. It must be

Crown Copyright © 2007

recognised that, because no knowledge exists a priori of ϵ and r values, both were determined empirically after some limited 'tuning' of the RP scheme. Finally, the parameters' values are equal for all grid points (i.e. the spatial correlation is 1).

4.2 The Stochastic Convective Vorticity (SCV) scheme

The main aim of the SCV scheme (Gray and Shutts, 2002) is to represent a Potential Vorticity (PV) anomaly dipole similar to the one typically associated with a Meso-scale Convective System (MCS). As shown in observational studies (Bartels and Maddox, 1991), MCSs possess an upper-level anticyclone, associated with the cirrus outflow or anvil, and also a smaller-scale mid-level cyclonic vortex near the freezing level. However, given that MCSs may be only partially resolved in the model as an area of parameterised convection, the PV dipole generated by them may be poorly represented. Consequently, the NWP model may not transfer as much of the sub-grid diabatic heating into resolved balanced motions as would be suggested from high-resolution modelling studies (Gray *et al.*, 1998). It has been also shown that PV anomalies associated with MCSs could have a significant impact on the forecast evolution, especially when located close to baroclinic zones (Gray, 2001; Beare *et al.*, 2003).

In the SCV scheme the PV dipole is formed by two vortices, one mid-level cyclone representing the positive PV anomaly and one upper-level anticyclone representing the negative PV anomaly, the scales of which are determined using a randomised function. Because the application of a PV anomaly through a PV inverter would make the scheme prohibitively expensive, a simpler approach, just modelling the vorticity part of the PV anomaly, was used. Also, it appears from Gray (2001), that the vorticity is more important in perturbing the forecast than the stratification, so this simplification is not expected to be detrimental to the overall impact of the scheme.

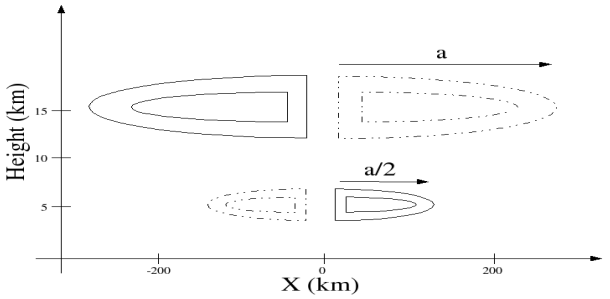

Figure 7. Stochastic convective vorticity adds a vorticity dipole, at mid-levels and at upper levels to model the effect of un-resolved convection on the resolved flow.

Schematically, the upper-level anticyclone is of depth d_a, centred at height z_a and consisting of a zero PV core of radius a. The mid-level cyclonic vortex is of depth d_c, centred at height z_c and is of radius ηa, where η is set as 0.5. Therefore, we have six parameters (see Figure 7), a, d_a, d_c, z_a, z_c, and η that determine the size, shape, position and magnitude of the vorticity dipoles. In implementing the SCV all six could be given some form of random element but, given that the size of the MCS, a, is clearly the parameter which has the largest range in the atmosphere and in order to simplify the SCV scheme for initial implementation, only a will vary stochastically. As suggested by Shutts (1987) a is related to the value of CAPE (Convective Available Potential Energy) according to the following formula:

$$a = \alpha R p_r \frac{\sqrt{CAPE}}{f} \tag{12}$$

where α is a tunable constant which was determined empirically to produce good agreement between

Crown Copyright © 2007

Parameter	Scheme	Min	std	Max
Entrainment rate coefficient	Convection	2	3	4
Cape timescale	Convection	30	30	60
Flux profile parameter	Boundary layer	5	10	20
Neutral mixing length	Boundary layer	0.05	0.15	0.5
Gravity wave constant	Gravity wave drag	7.5×10^4	10^5	1.33×10^5
Froude number	Gravity wave drag	2	4	4
Critical relative humidity	Large-scale precipitation	0.875	0.9	0.925
Ice fall speed	Large-scale precipitation	17	25.2	33

Table I. Parameters included in the RP scheme. The physical parameterisation of which they are part is indicated in the second column. The third and fifth columns indicate the minimum and maximum limits for the value of the parameter and the fourth column gives the parameter's value as in the standard setting of the Met Office Unified Model version 6.0.

simulated and observed frequency and size of MCSs. A value of 0.1 was found to produce satisfactory results. R is a random number taken from a uniform distribution [0,1] and p_r is the diagnosed convective precipitation, which provides a link to the convection scheme in the model and makes a proportional to the magnitude of the diagnosed convective rain rate. f is the Coriolis parameter. It must be noted that as $f \to 0$ at the Equator $a \to \infty$; to avoid this, f is assigned a minimum value of 2 x $10^{-5}s^{-1}$.

4.3 Impact of Stochastic Physics

It is important to remark that the main role of the stochastic physics is not to generate noise to increase the spread in the ensemble but to truly represent the model uncertainties in the system. Therefore, attention is needed to verify that these schemes are able to change the forecast while at the same time not degrading the quality of the model. In order to check this, the RP and SCV schemes have been tested in a series of 5-day forecast case study runs (similar to those typically used to test new developments in parameterisations) and as part of a 3-year climate run.

The case study runs include 10 5-day forecasts from the JJA 2003 and DJF 2003-2004 period.

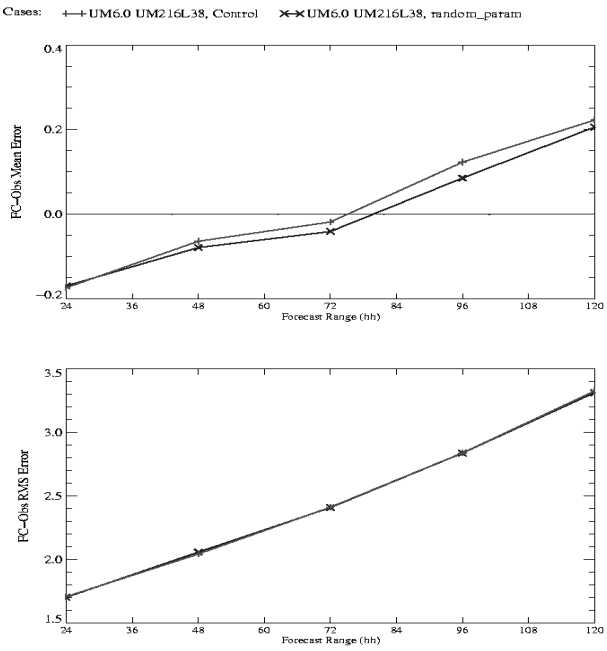

Figure 8. Bias (top) and rms-error (bottom) for temperature at 850 hPa verified against radiosonde observations for the Northern Hemisphere (20N-90N). The red line corresponds to the control run and the blue line to the stochastic physics run.

These forecasts were completed using a configuration of the UM similar to the operational model with a horizontal resolution of N216 and 38 levels in the vertical, without data assimilation. An example of the results from these short-range forecasts is shown in Figure 8 (temperature at 850 hPa for the control and stochastic physics run verified against radiosonde observations for the Northern Hemisphere, 20N-90N) and in Figure 9 (mean sea level pressure

Crown Copyright © 2007

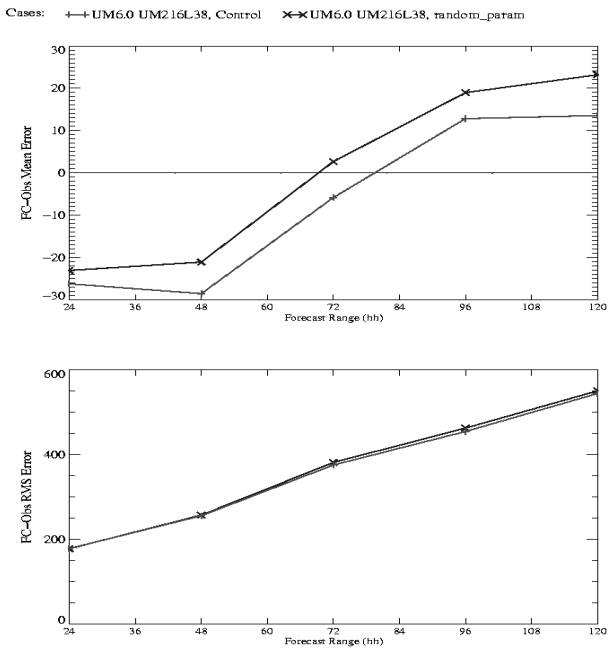

Figure 9. Bias (top) and rms-error (bottom) for mean sea level pressure verified against surface observations for the Northern Hemisphere (20N-90N). The red line corresponds to the control run and the blue line to the stochastic physics run.

for control and stochastic physics verified against surface observations for the Northern Hemisphere, 20N-90N). In both figures biases are shown in the upper panel and root mean square errors in the bottom panel. As can be seen, differences between the control and the stochastic physics run are small. Similar results are seen for other variables, regions and verification times. Therefore, the skill (compared to a standard version of the model) of the Met Office Unified Model when the stochastic physics schemes are included does not change significantly in the short-range.

Additionally, two 3-year simulations, a control run and a run including the RP and SCV schemes, were completed using HadGAM1, the atmosphere-only climate version of the Unified Model (Ringer *et al.*, 2006). Although three years is too short for a full quantitative analysis of climate differences between the two runs, it is long enough to spot any significant systematic changes that the presence of the stochastic schemes may cause. Both simulations were evaluated using the Climate Prediction Index (Murphy *et al.*, 2004), which was developed to measure how well a climate model reproduces various aspects of the climate system such as atmospheric radiation and clouds, atmospheric dynamics or the hydrological cycle. A complete list of all variables analysed can be found on the x-axis in Figure 10. For all simulated seasonal means each variable is compared against the appropriate observational or re-analysis data set. As shown in Figure 10, model performance is similar for all variables. The (averaged over all variables) CPI values for both simulations are 2.46 for Control and 2.52 for the stochastic physics run, showing that both simulations are providing similar-quality representations of the current climate.

We can conclude then that the stochastic schemes are having a neutral impact on the model climate and short-range weather forecasting skill. Nevertheless, the stochastic physics schemes are able to have a substantial impact on an individual forecast. An example of this is given in Figure 11 which shows the changes in 2-m temperature and precipitation in a 72-h forecast over the UK region with respect to a control simulation with no stochastic physics schemes. As can be seen, the schemes are able to produce a sharply cooler forecast of 2m temperature over England. This is mainly produced by the impact of the RP scheme in the boundary layer parameterisation, introducing changes between a diagnosed stable or unstable boundary layer.

Crown Copyright © 2007

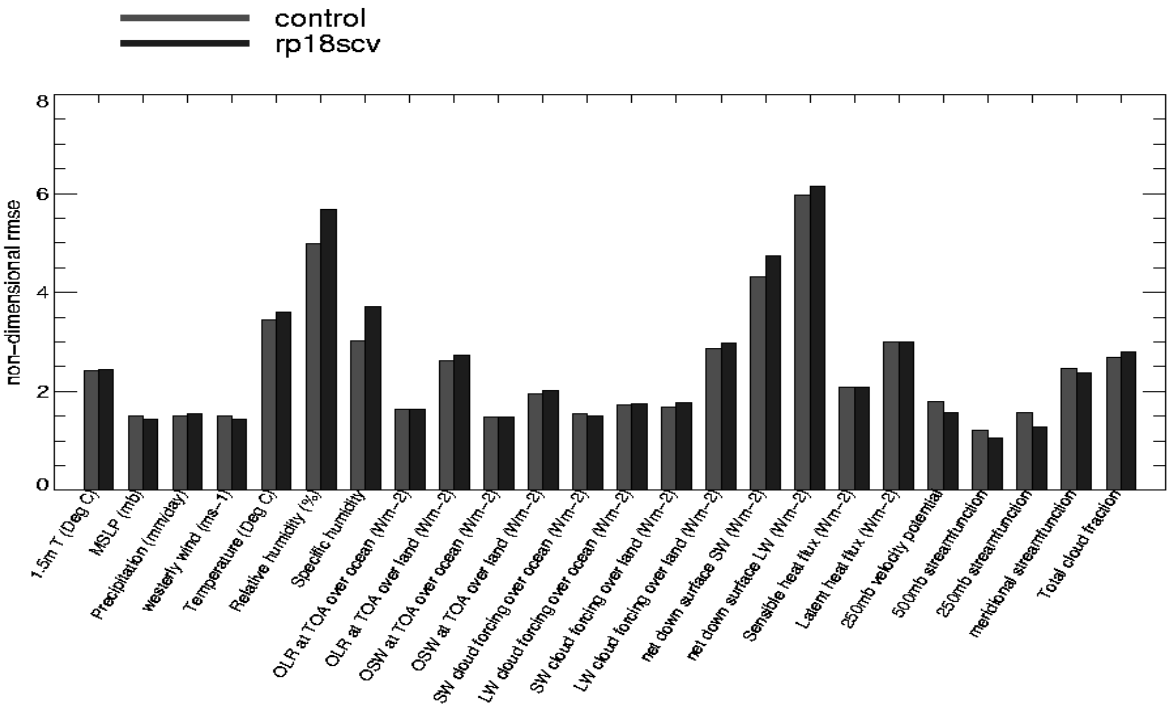

Figure 10. The climate prediction index for a control run, and a run using the random parameters scheme. The overall performance of the both runs is similar.

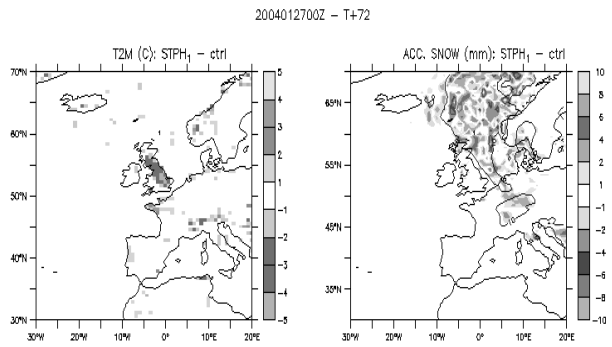

Figure 11. The difference in 2m temperature and snow accumulation forecast from a control run and a run with stochastic physics. The perturbed forecast gives much lower temperatures over the UK and a slight increase in the southward penetration of snow.

5 Summary and Conclusions

In this paper we have described the setup of the MOGREPS system, a global and regional ensemble for short-range forecasting (0-3 days). The global ensemble calculates its initial condition perturbations using the ETKF, which includes all the observations assimilated by the 4D-Var analysis system used at the Met Office. The regional ensemble runs 6 hours later than the global ensemble, and takes its initial condition perturbations directly from the global model.

Both the global and regional ensembles use stochastic physics schemes to perturb the model evolution. The random parameters scheme is used in both ensembles and involves perturbing various tunable parameters used in the parameterisation of sub-grid-scale processes. The stochastic convective vorticity scheme, used in the global ensemble, introduces a vorticity dipole in the region of severe convection to mimic the effect of meso-scale convective systems.

Future upgrades to MOGREPS include a localised version of the ETKF, the use of the ETKF to calculate initial condition perturbations specifically

Crown Copyright © 2007

for the NAE model and the introduction of a stochastic kinetic energy backscatter scheme to better represent model uncertainties. Details of the performance of MOGREPS are dealt with in the following paper.

6 Acknowledgements

The development of the MOGREPS system has depended on the input of many people within the Met Office, and we would like to thank all those who have been involved. In particular, we thank Adam Maycock, Sarah Beare, David Goddard, Tim Legg, Iain Anderson and David Sexton for their involvement.

References

Alhamed, A., Lakshmivarahan, S., and Stensrud, D.J., "Cluster Analysis of Multimodel Ensemble Data from SAMEX", *Monthly Weather Review*, **130**, 226-256 (2002)

Arribas, A., Robertson, K. B. and Mylne, K. R., "Test of a Poor Man's Ensemble Prediction System for Short-Range Probability Forecasting", *Monthly Weather Review*, **133**, 1825-1839 (2005)

Bartels, D.L. and Maddox, R.A., "Midlevel cyclonic vortices generated by mesoscale convective systems", *Monthly Weather Review*, **119**, 104-118 (1991)

Beare, R.J., Thorpe, A.J. and White, A.A., "The predictability of cyclones: non-linear sensitivity to localised potential vorticity perturbations", *Quarterly Journal of the Royal Meteorological Society*, **129**, 219-237 (2003)

Bishop, C.H., Etherton, B.J. and Majumdar, S.J., "Adaptive sampling with the ensemble transform kalman filter. Part 1: theoretical aspects", *Monthly Weather Review*, **129**, 420-436 (2001)

Bowler, N.E., "Comparison of error breeding, singular vectors, random perturbations and ensemble Kalman filter perturbation strategies on a simple model", *Tellus*, **58A**, 538-548 (2006)

Bozic, S.M., "Digital and Kalman Filtering", *Edward Arnold (Publishers) Ltd*, Bedford Square, London (1979)

Bright, D.R. and Mullen, S.L., "Short-range ensemble forecasts of precipitation during the southwest monsoon", *Weather and Forecasting*, **17**, 1080-1100 (2002)

Buizza, R., Houtekamer, P.L., Toth, Z., Pellerin, G., Wei, M., and Yuejian Z., "A comparison of the ECMWF, MSC and NCEP global ensemble prediction systems", *Monthly Weather Review*, **133**, 1076-1097 (2005)

Buizza,R. and Palmer,T.N., "The singular-vector structure of the atmospheric general circulation" *J. Atmos. Sci.*, **52**, 1434-1456 (1995)

Eckel, F.A. and Mass, C.F., "Aspects of effective mesoscale, short-range ensemble forecasting" *Weather and Forecasting*, **20**, 328-350 (2005)

Evensen, G., "Sequential data assimilation with a nonlinear quasi-geostrophic model using monte-carlo methods to forecast error statistics", *Journal of Geophysical Research - Oceans*, **99 (C5)**, 10143-10162 (1994)

Evensen, G., "Sampling strategies and square root analysis schemes for the EnKF", *Ocean Dynamics*, **54 (6)**, 539-560 (2004), see also

Crown Copyright © 2007

http://enkf.nersc.no/Publications/eve04a_typos.pdf for errata.

Frogner, I-L., Haakenstad, H. and Iversen, T., "Limited-area ensemble predictions at the Norwegian Meteorological Institute", *Quarterly Journal of the Royal Meteorological Society*, **132**, 2785-2808 (2006)

Garcia-Moya, J.A., Callado, A., Santos, C., Santos, D. and Simarro, J., "The role of mass transfer in describing the dynamics of mesoscale convective systems", *3rd International Verification Methods Workshop*, ECMWF, (2007) (http://www.ecmwf.int/newsevents/meetings/workshops/2007/jwgv/workshop_presentations/index_poster.htm)

Gray, M.E.B., Shutts, G.J. and Craig, G.C., "The role of mass transfer in describing the dynamics of mesoscale convective systems", *Quarterly Journal of the Royal Meteorological Society*, **124**, 1183-1207 (1998)

Gray, M.E.B., "The impact of mesoscale convective system potential vorticity anomalies on numerical weather prediction forecasts", *Quarterly Journal of the Royal Meteorological Society*, **127**, 73-88 (2001)

Gray, M.E.B. and Shutts, G.J., "A stochastic scheme for representing convectively generated vorticity sources in general circulation models", *APR Turbulence and Diffusion Note No. 285*, Met Office, UK (2002)

Gregory, D. and Rowntree, P.R., "A mass flux convection scheme with representation of cloud ensemble characteristics and stability-dependent closure" *Monthly Weather Review*, **118**, 1483-1506 (1990)

Hamill, T.M. and Colucci, S.J., "Verification of eta-RSM short-range ensemble forecasts", *Monthly Weather Review*, **125 (6)**, 1312-1327 (1997)

Houtekamer, P.L., Lefaivre, L. and Derome J., "The RPN ensemble prediction system" in *Vol. II of Proceedings of the seminar on predictability*, ECMWF, Reading, Berkshire, UK, 121-146 (1995)

Houtekamer, P.L. and Mitchell, H.L., "Data assimilation using an ensemble Kalman filter technique", *Monthly Weather Review*, **126**, 796-811 (1998)

Kalman, R.E., "A new approach to linear filtering and prediction problems", *Transactions of the AMSE - Journal of Basic Engineering*, **82 D**, 35-45 (1960)

Lin, J.W.B. and J.D. Neelin, "Influence of a stochastic moist convective parameterization on tropical climate variability", *Geophysical Research Letters*, **27**, 3691-3694 (2000)

Lock, A.P., Brown, A.R., Bush M.R., Martin, G.M. and Smith, R.N.B, "A new boundary layer mixing scheme. Part I: Scheme description and single column model tests", *Monthly Weather Review*, **128**, 3187-3199 (2000)

Marsigli C., Boccanera F., Montani A. and Paccagnella T., "The COSMO-LEPS mesoscale ensemble system: validation of the methodology and verification", *Nonlinear Processes In Geophysics*, **12 (4)**, 527-536 (2005)

Marsigli C., Montani A., Nerozzi F. and Paccagnella T., "Probabilistic high-resolution forecast of heavy precipitation over Central Europe" *Natural Hazards And Earth System Sciences*, **4 (2)**, 315-322 (2004)

Molteni,F., Buizza,R., Palmer,T.N. and Petroliagis,T., "The ECMWF Ensemble Prediction System:

Crown Copyright © 2007

Methodology and Validation" *Quarterly Journal of the Royal Meteorological Society*, **122**, 73-119 (1996)

Molteni F., Buizza R., Marsigli C., Montani A., Nerozzi F. and Paccagnella T., "A strategy for high-resolution ensemble prediction. I: Definition of representative members and global-model experiments" *Quarterly Journal of the Royal Meteorological Society*, **127 (576)**, 2069-2094 (2001)

Murphy J.M., Sexton, D.H., Barnett, D.N., Jones, G.S., Webb, M.J., Collins, M. and Stainforth, D.A., "Quantification of modelling uncertainties in a large ensemble of climate change simulations" *Nature*, **430**, 768-772 (2004)

Ringer, M.A., Martin, G.M., Greeves, C.Z., Hinton, T.J., James, P.M., Pope, V.D., Scaife, A.A., Stratton, R.A., Inness, P.M., Slingo, J.M., Yang, G.-Y., "The Physical Properties of the Atmosphere in the New Hadley Centre Global Environmental Model (HadGEM1). Part II: Aspects of Variability and Regional Climate" *J. Climate*, **19**, 1302-1326 (2006)

Shutts, G. J., "Balanced flow states resulting from penetrative, slantwise convection", *Journal of the Atmospheric Sciences*, **44**, 3363-3376 (1987)

Stensrud DJ, Brooks HE, Du J, Tracton MS, Rogers E, "Using ensembles for short-range forecasting", *Monthly Weather Review*, **127**, 433-446 (1999)

Toth,Z. and Kalnay,E., "Ensemble Forecasting at the NMC: The generation of perturbations", *Bull. Amer. Meteor. Soc.*, **74**, 2317-2330 (1993)

Tracton M. S., Du J., Toth Z. and Juang H., "Short-range ensemble forecasting (SREF) at NCEP/EMC" *12th Conf. on Numerical Weather Prediction, Phoenix*, American Meteorological Society, 269-272 (1998)

Whitaker, J.S. and Hamill, T.M., "Ensemble data assimilation without perturbed observations" *Monthly Weather Review*, **130**, 1913-1924 (2002)

Wang, X.G. Bishop, C.H., "A comparison of breeding and ensemble transform Kalman filter ensemble forecast schemes" *Journal of the Atmospheric Sciences*, **60**, 1140-1158 (2003)

Wang, X.G., Bishop, C.H. and Julier S.J., "Which is better, an ensemble of positive-negative pairs or a centered spherical simplex ensemble?" *Monthly Weather Review*, **132**, 1590-1605 (2004)

Webster, S., Brown, A.R., Cameron, D.R. and Jones, C.P., "Improvements to the representation of orography in the Met Office Unified Model", *Quarterly Journal of the Royal Meteorological Society*, **129**, 1989-2010 (2003)

Wei, M.Z., Toth, Z., Wobus, R., Zhu, Y.J., Bishop, C.H. and Wang X.G., "Ensemble transform Kalman filter-based ensemble perturbations in an operational global prediction system at NCEP" *Tellus*, **A 58**, 28-44 (2006)

Wilks, D.S., "Statistical methods in the atmospheric sciences - an introduction", *International Geophysics Series*, **59**, Academic Press, New York, USA, (1995)

Wilson, D.R. and Ballard, S.P., "A microphysically based precipitation scheme for the UK Meteorological Office Unified Model", *Quarterly Journal of the Royal Meteorological Society*, **125**, 1607-1636 (1999)

Crown Copyright © 2007